



Finite Size Effects in Carbon Nanotubes

著者	川添 良幸
journal or publication title	Applied Physics Letters
volume	77
number	16
page range	2554-2556
year	2000
URL	http://hdl.handle.net/10097/46992

doi: 10.1063/1.1318241

Finite size effects in carbon nanotubes

Jian Wu,^{a)} Wenhui Duan, and Bing-Lin Gu

Center for Advanced Study, Tsinghua University, Beijing 100084, People's Republic of China and
Institute for Materials Research, Tohoku University, Sendai 980-8577, Japan

Jing-Zhi Yu and Yoshiyuki Kawazoe

Institute for Materials Research, Tohoku University, Sendai 980-8577, Japan

(Received 30 May 2000; accepted for publication 23 August 2000)

The low-energy theory for finite long carbon nanotube is derived and numerically examined. It shows that the electronic structure is dominated by the quantum confining, which determines the profile of wave functions as well as the eigen energies; while the details of the wave functions are resolved by the structure of the nanotubes. This behavior is attributed to the peculiar electronic structure of the nanotubes. Because of the slow variation of the profile of electron wave functions, the measured conductance is NOT independent of the position to measure it, which is evident in the multiprobe experiment. © 2000 American Institute of Physics. [S0003-6951(00)01542-4]

Carbon nanotubes are nanoscale molecules obtained by wrapping graphitic layers to seamless cylinders, and are typically longer than a micrometer, with diameters ranging from 1 to 20 nm.¹ The discovery of single-walled carbon nanotubes (SWNTs)² has prompted numerous studies on these exotic materials, because they would allow a much better comparison with theory than would the multiwalled nanotubes. It has been theoretically predicted³ and experimentally confirmed⁴ that a SWNT could be a metal, a semimetal, or an insulator, depending on the tube diameter and wrapping angle, which can be characterized by a pair of integer indices (n, m) of the wrapping superlattice vector with $0 \leq m \leq n$. Since the first transport measurements on a SWNT was reported in 1997,⁵ the finite size effects in carbon nanotubes have attracted many interests. It is well known that limiting the length of a SWNT will lead to a "particle-in-a-box" quantization of the energy levels and result in the standing wave (SW) characteristic in the wave functions. Remarkably, the electronic wave functions were recently reported to be observed in short (10,10) carbon nanotubes by scanning tunneling microscopy (STM).⁶

Here we report that, contrary to conventional consideration, the length limitation in carbon nanotubes may result in peculiar characteristics of energy levels, eigen-wave functions, and transmission properties. We focus on the armchair SWNTs which were used in most of the recent experiments.

In order to give a clear picture on physics, a tight-binding (TB) representation of the electron states is used to model the finite long carbon nanotubes in the numerical treatment. The real space Green's function method⁷ is employed to calculate the local density of states (LDOS). By attaching 2 one-dimensional (1D) ideal leads to the finite system from both sides, we calculate the conductance through the system with the linear-response approach.⁸ Figure 1 shows the conductance through the nanotube as a function of its static potential (energy), which is introduced by the gate voltage in the experiments, in a (10,10) nanotube with 1139 atomic tube layers, which corresponds to the 140-nm-long tube between the electrodes in a recent experiment.⁵

And the density of states (DOS) is plotted as a reference. In general, a discrete electron level that is aligned with the Fermi energy E_f of the electrodes will cause resonant tunneling through the tube and result in conductance peaks. It is interesting to find that in Fig. 1, a conductance minimum is shown clearly to be simultaneous with the maximum of the DOS. While the doubling of the conductance peaks, rather than simple sequent peaks, is just the phenomenon observed in the experiment.⁵ In order to give more insights of this phenomenon, the LDOS patterns for the two lowest energy levels above the Fermi level are calculated and shown in Fig. 2.

An armchair SWNT has a periodicity $a = 0.246$ nm along the tube axis. The Fermi level is at $k_F = 2\pi/3a$, where the direction of k_F is along the tube axis. In a 1D particle-in-a-box model, the electron eigenstates ("allowed" states) of a SWNT with length L are SW of the form $\sin(kx)$, with

$$k = m\pi/L \quad (1)$$

and m being integer. It is usually derived that, near the Fermi energy E_F , the allowed states are restricted to k points that satisfy Eq. (1)⁹ with $k \approx k_F$. This, however, obviously does

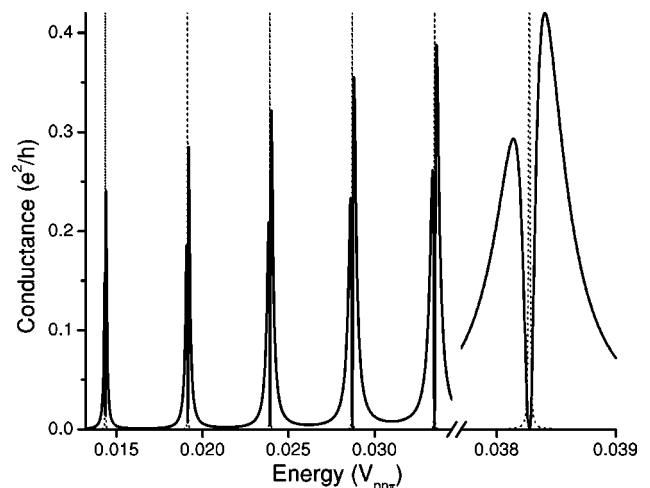


FIG. 1. Conductance (in units of e^2/h) as a function of the energy. DOS is plotted as a reference by the dotted line. The region near $E = 0.038 V_{pp}$ is enlarged as an example to show the detail.

^{a)}Electronic mail: wj@phys.tsinghua.edu.cn

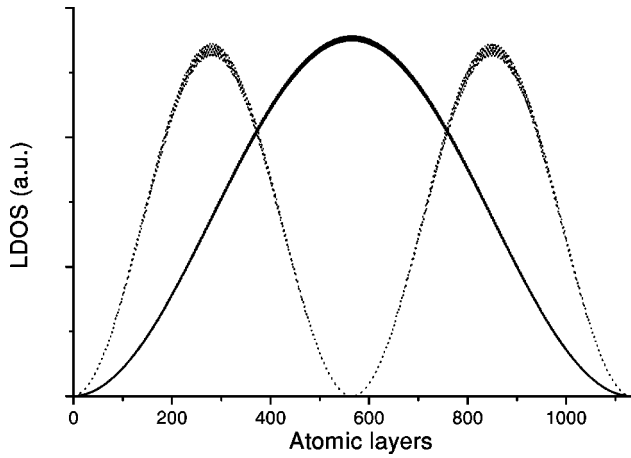


FIG. 2. Comparison of LDOS for the two lowest energy levels in the nanotube with 1139 atomic tube layers. The solid and dotted curves correspond to the first and second lowest energy levels, respectively.

not accord with the results shown in Fig. 2. Moreover, our numerical result suggests a more reasonable form of the eigen-wave functions: $\sin(\Delta kx)\phi(k_Fx)$ with the modulation of $\phi(k_Fx)$ being a slowly varied function and $\Delta k \ll k_F$.

The profound difference between this finite size problem and conventional particle-in-a-box one is that there exist two bands crossing the Fermi level with

$$E(k_F + \Delta k) = E(k_F - \Delta k), \quad (2)$$

which is due to the existence of two sublattices in nanotubes. A more general presentation of the above equation can be expressed as $E(k_F + k_1) = E(k_F - k_2)$ with $(0 < k_1, k_2 \ll k_F)$. This, however, can also be written in the form of Eq. (2) by defining $k'_F = k_F + (k_1 - k_2)/2$, while the “Fermi wave vector” k'_F may be shifted slightly from the exact value of $2\pi/3a$. It will be shown (see below) that this shift of k_F is very small, about one order smaller than Δk (so we have $k'_F \approx k_F$). As a result, at any energy $E = E(k'_F \pm \Delta k)$ the possible form of the wave function is

$$\psi(x) = e^{i(k'_F + \Delta k)x} + c e^{i(k'_F - \Delta k)x} \quad (3)$$

with the x axis along the tube direction, and c a constant. Considering the 1D quantum box boundary condition, we obtain $c = -1$ and

$$\psi(x) = \sin(\Delta kx) e^{ik'_Fx} \quad (4)$$

with

$$\Delta k = m\pi/L \quad (5)$$

and m being integer no matter whether k'_F is or is not the “allowed” state of the nanotube. Moreover, noting that the derivative of the wave function specialized above [$O(\Delta k)$] tends to be zero near the boundary, we find that $\psi(x)$ satisfies the more restricted boundary condition, i.e., the continuity of the derivative of the wave function. This condition is obviously not satisfied by the conventionally considered allowed states in the form of $\sin[(k_F + \Delta k)x]$.

The boundary effects could be crucial in a short nanotube. Therefore, before a full consideration of the boundary effects, we first focus on the simpler case: a nanotube with enough long length, for which the boundary effects can be

neglected. In this case, the low eigen energy can be easily calculated using the usual TB model ($E_F = 0$) as

$$E/V_{pp\pi} = \pm \frac{\sqrt{3}}{2} \Delta ka \mp \frac{1}{8} (\Delta ka)^2 + O[(\Delta k)^3], \quad (6)$$

where $V_{pp\pi}$ is the nearest-neighbor interaction energy between p_z orbitals oriented perpendicular to the tube axis. And these low energy states are degenerate. It has been pointed out that the degeneracy of energy levels may result in antiresonances for which the conductance g tends to zero⁸ at the center of the energy level. Consequently, the conductance peaks through a nanotube at the allowed states will split, with the center of the two split peaks corresponding to the energy level. The transport measurement experiment on a totally 3- μm -long (10,10) nanotube⁵ is just the case. The doubling of the conductance peaks was observed in this experiment, and accords with our numerical results.

The LDOS patterns shown in Fig. 2 indicate that the profile of wave function is indeed in the form of $\sin(\Delta kx)$, as given in Eq. (4). The small oscillation of the LDOS in the figure is caused by the boundary effects. Therefore, it opens a route to experimentally observe the macroquantum-wave caused by the quantum confining in nanotubes.

Let us consider a more realistic model corresponding to the nanotubes in experiments by taking the boundary effects into account. There should definitely exist some structural defects, in comparison with the perfect periodic boundary condition, including suspensive bonds of carbon atoms, pentagons, and so on. The localized states induced by the defects will, obviously, not affect the electronic transmission properties much, which is attributed mainly to the extended states. However, the potential profile at the boundary layers, or at the defects, is different from the inner ones. In other words, some interim layers, where an additional static potential is considered, should be included between the periodic structure and boundary in the simple quantum box model. Hence the distribution of the wave function within these layers should contribute a small additional energy to the energy level. It is easy to find that the degenerate states expressed by Eq. (4) will split to two nondegenerate states:

$$\psi(x) = \sin(\Delta kx) \cos k'_Fx \quad \text{and} \quad \sin(\Delta kx) \sin k'_Fx. \quad (7)$$

There is slightly a difference between the energy of these two states because of different distribution of their wave functions within the interim layers. While for a longer nanotube, the energy difference between the two nondegenerate states is so small that they are mixed again to form approximately degenerate states. However, these states are only the mixture of the states, without exact degeneracy. This results in the small oscillation of the LDOS in Fig. 2.

The similar numerical study on a shorter (10,10) nanotube with 243 atomic tube layers, which corresponds to the 30-nm-long tube in a recent experiment,⁶ is performed to verify the above analysis. Because of the shorter length, the suspensive bonds of carbon atoms at boundary should contribute more to the electronic states. As expected, the energy levels are found to be in pairs, and the profiles of the wave functions for each pair of energy levels are in the same form of $\sin(\Delta kx)$ with $\Delta k = m\pi/L$ ($m = 1, 2, 3, \dots$). The LDOS pattern for a pair (the two lowest) of energy levels above the

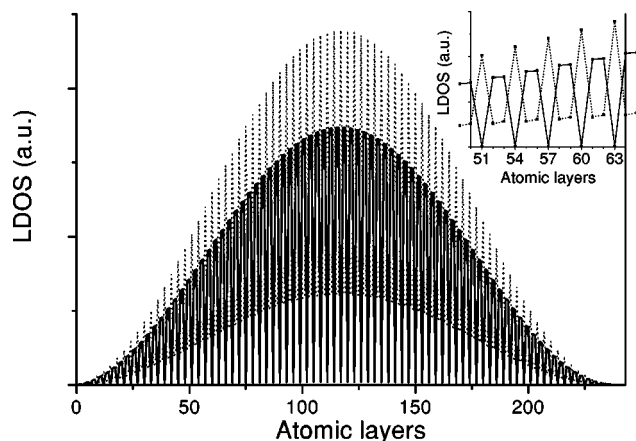


FIG. 3. LDOS for the two lowest energy levels in the nanotube with 243 atomic tube layers. The solid and dotted curves correspond to the first and second lowest energy levels, respectively. Part of the figure is enlarged as the inset, where the calculated values are given as marks. The lines in the inset are given as a guide.

Fermi level is shown in Fig. 3: the high frequency components are in the form of $\sin(k'_F x + \theta)$ with $k'_F \approx 2\pi/3a$ (see inset), and there exists a phase difference of $\Delta\theta = \pi/2$ between the two states. It is obvious that either one corresponds to one of the wave functions expressed in Eq. (7).

Below a brief discussion is given on the results in the recent experiments.^{5,6,10} Because the STM tip in the experiment⁶ was scanned within only a very short range (about 2 nm), which corresponds to only 10–20 atomic tube layers in the nanotube, the slowly modulation $[\sin(\Delta kx)]$ is invisible in this experiment. As a result, only the wave-vector corresponding the high frequency components, the k'_F in Eq. (7), can be observed and measured. By considering the small departure of the TB model from the real system, the measured value of k'_F may be slightly different from $2\pi/3a$. The difference of k'_F between two energy levels should be much smaller than its shift from $2\pi/3a$. Moreover, depending on the position x_0 of the STM tip or the electrodes, some energy levels could also be invisible while $\sin(\Delta kx_0)$ is close to zero. It should be noted that the wavelength of the slowly varied modulation is so long, i.e., comparable with the length of the tube, that this wave node phenomenon may occur through nanometers wide, as the size of electrodes. Therefore, the equal-splitting energy behavior may not be observed in the experiments.^{5,6,10} Furthermore, it should be mentioned that the peculiar conductance behavior (i.e., the conductance measured between adjacent pairs of electrodes are similar but not identical) in the multiple nanoelectrodes experiment on an individual SWNT¹⁰ may also be caused by the position dependent characteristic in finite size nanotubes. For some energy levels, the electron distribution at some electrodes tends to zero, so the measured conductance through it may decrease greatly, and then no conductance peaks can be observed in these energy levels. As a result, the conductance measured between a pair of electrodes shows only parts of the energy level pattern, while the combination of the conductance pattern measured between different pairs of electrodes will give a more complete view of the energy levels in the SWNT. Obviously the combined conductance pattern in the experiment¹⁰ did show almost equal-splitting energy levels. Figure 4 shows the conductance pattern calculated between different positions in a (10,10) armchair nano-

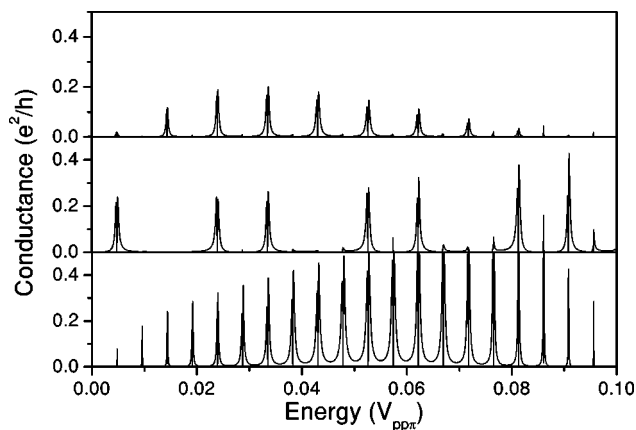


FIG. 4. Conductance pattern calculated at different positions in a (10,10) armchair nanotube with 1139 atomic tube layers.

tube with 1139 atomic tube layers. At a definite energy level, there will be no conductance peak if an electrode is close to a node of the corresponding wave function. The results are in good agreements with the above analysis. It can also be classified to the interference effects, as what was pointed out by us in the mesoscopic ring system.¹¹

In conclusion, the finite size effects in armchair carbon nanotubes are presented. We find that the low-energy electronic structure of a finite long carbon nanotube can be given by a generalized “particle-in-a-box” model, i.e., the electronic structure is dominated by the quantum confining, which determines the profile of the wave functions as well as the eigen energies; while the peculiar electronic distribution is resolved by the structure of the nanotubes. This striking behavior is attributed to the peculiar electronic structure of the nanotubes, i.e., two bands intersect the Fermi level. Moreover, because of the slow variation of the electron distribution, the measured conductance, probably along with some other related measurable physical properties, are NOT independent of the position to measure them, which is the reason why the tube did “not” behave as one continuous quantum wire with extended quantum states in a multiprobe transport experiments.¹⁰

This work is partly supported by the High Technology Research and Development Program of China.

¹T. W. Ebbesen, Phys. Today **49**, 26 (1996).

²S. Iijima and T. Ichihashi, Nature (London) **363**, 603 (1993); D. S. Bethune, C. H. Kiang, M. S. de Vries, G. Goreman, R. Savoy, J. Vazquez, and R. Beyers, *ibid.* **363**, 605 (1993).

³J. W. Mintmire, B. I. Dunlap, and C. T. White, Phys. Rev. Lett. **68**, 631 (1992); N. Hamada, S. Sawada, and A. Oshiyama, *ibid.* **68**, 1579 (1992).

⁴J. W. G. Wildöer, L. C. Venema, A. G. Rinzler, R. E. Smalley, and C. Dekker, Nature (London) **391**, 59 (1998); T. W. Odom, J. L. Huang, P. Kim, and C. M. Lieber, *ibid.* **391**, 62 (1998).

⁵S. J. Tans, M. H. Devoret, H. Dai, A. Thess, R. E. Smalley, L. J. Geerligs, and C. Dekker, Nature (London) **386**, 474 (1997).

⁶L. C. Venema, J. W. G. Wildöer, S. J. Tans, J. W. Janssen, L. J. Hinne, T. Tuinstra, L. P. Kouwenhoven, and C. Dekker, Science **282**, 52 (1999).

⁷H. Chen, J. Wu, Z. Q. Li, and Y. Kawazoe, Phys. Rev. B **55**, 1578 (1997); Phys. Lett. A **240**, 241 (1998).

⁸A. Aldea, P. Gartner, and I. Corcoroti, Phys. Rev. B **45**, 14122 (1992).

⁹For example, see A. Rubio, D. Sánchez-Portal, E. Artacho, P. Ordejón, and J. M. Soler, Phys. Rev. Lett. **82**, 3520 (1999).

¹⁰A. Bezryadin, A. R. M. Verschueren, S. J. Tans, and C. Dekker, Phys. Rev. Lett. **80**, 4036 (1998).

¹¹J. Wu, B. L. Gu, H. Chen, W. Duan, and Y. Kawazoe, Phys. Rev. Lett. **80**, 1952 (1998).